THE JOURNAL OF PHYSICAL CHEMISTRY LETTERS
A JOURNAL OF THE AMERICAN CHEMICAL SOCIETY

pubs.acs.org/JPCL Letter

# The Solvation Entropy of Different Simulation Models of the Hydrated Electron

William R. Borrelli, Xiaoyan Liu, and Benjamin J. Schwartz*

Cite This: https://doi.org/10.1021/acs.jpclett.5c02808 Read Online

ACCESS | Metrics & More | Article Recommendations | Supporting Information

**ABSTRACT:** Understanding the solvation structure of the hydrated electron, an excess electron in bulk water, has been a long-standing challenge. Experiments have shown that the solvation entropy, which encodes how the water molecules near the electron behave, is anomalously large and positive for the hydrated electron. Here, we use semiclassical and *ab initio* alchemical simulations to calculate the solvation entropy of several simulation models of the hydrated electron, including *ab initio* density functional theory (DFT) with a hybrid GGA functional. We find that cavity-forming one-electron models with relatively soft cavities correctly predict the sign of the hydrated electron's solvation entropy but underestimate its magnitude. Both a noncavity one-electron model and hard cavity-forming DFT yield an incorrect sign for the solvation entropy. The calculated solvation entropies of each model are consistent with the structure and dynamic behavior of the first-shell waters molecules.

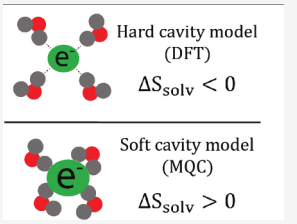




Excess electrons in liquid water form stable species called hydrated electrons. These nominally simplest of anions have been the topic of active research since their discovery,[1] including investigations of their fundamental behavior, powerful reducing strength,[2] and anomalous chemical reactivity.[3−6] Despite decades of experimental[7−9] and theoretical[2,3,9−15] research, however, there is still no definitive characterization of the structure of this species; that is, we still do not know definitively how the structure of liquid water changes in the presence of an excess electron, or how much of the excess charge is donated onto the first-shell water molecules. The structure of the waters surrounding the hydrated electron ($e^-_{hyd}$) is intimately connected to its reactivity; for example, the way waters are organized may explain why the Marcus theory of electron transfer[16] fails for reactions involving hydrated electrons.[17]

Early theoretical work viewed the hydrated electron as a charge defect localized to a cavity in bulk water,[18] a perspective that has been corroborated by one-electron molecular dynamics (MD) simulations in which the interaction between the quantum electron and the classical water is described by a pseudopotential.[19,20] In 'cavity-forming' one-electron models, the excess charge density occupies a roughly spherical space in bulk water into which water molecules do not penetrate, so the $e^-_{hyd}$ behaves approximately as a particle in a spherical box.[2,21,22] In 2010, our group introduced a noncavity-forming one-electron model of the hydrated electron that was in good agreement with experiment for many observables.[2,10] However, the consensus of further theoretical work has concluded that a cavity model is more consistent with most experimental results for this object. Despite this consensus, no single model is able to match with experiment across the board. This is because not all cavity-forming models of the $e^-_{hyd}$ are equivalent, as each model yields different solvation structures and thus different predictions of experimental observables.

In recent years, *ab initio* quantum chemistry calculations based on density functional theory (DFT) have become tenable for small hydrated electron simulations.[11,12,14,23] Most such DFT-based simulations use the PBE0-D3 level of theory;[11,12,24] the $e^-_{hyd}$ simulated this way also occupies a cavity,[11,14] but the cavity is smaller and has much more structured positions of the surrounding water molecules than is typical in one-electron simulations.[14] We refer to the PBE0-D3-simulated $e^-_{hyd}$ structure as a 'hard' cavity because of the limited fluctuations of the surrounding water molecules compared to the 'softer' cavities seen in most one-electron simulations.[23]

We note that because DFT is an *ab initio* theory, simulations of the $e^-_{hyd}$ are still quite limited in size (tens of water molecules) and duration (≤25 ps). Despite this, machine-learned interatomic potentials have been used to alleviate these limitations to some extent,[25−27] and recent work has shown that the solvation structure of the PBE0-D3-based hydrated electron does not change much going from 128 to 256 water molecules.[28] DFT is also susceptible to density-driven errors depending on the functional being used, an issue that is particularly important for anionic systems with diffuse charge density such as the hydrated electron.[29] Although the results

Received: September 10, 2025
Revised: December 11, 2025
Accepted: December 12, 2025

presented here are only for the PBE0 functional, we have previously shown that the solvation structure of the hydrated electron is quite insensitive across a half-dozen functionals spanning many rungs of 'Jacob's Ladder'.[24,30]

All of this leads to the main question to be addressed in this paper: what local hydration structure and degree of fluctuations makes the most sense in explaining the physical properties and chemical reactivity of the $e^-_{hyd}$? We answer this question by explicitly calculating the solvation entropy for three one-electron models as well as DFT-based simulations of the hydrated electron using the PBE0 hybrid exchange-correlation functional with the D3 dispersion correction.

The solvation entropy ($\Delta S_{solv}$) is a thermodynamic quantity that quantifies how the translational and rotational degrees of freedom of the solvent are impacted by the presence of a solute. Experiments have shown that the hydrated electron has a solvation entropy of +124.6 J/mol·K,[31] a remarkably high value for a small ion in solution. The large positive value implies that the hydrated electron behaves like a hydrophobic ion that does not strongly orient or restrict the motions of nearby water molecules, but instead allows them to move more freely relative to water molecules in the bulk.[32] Interestingly, new experimental spectroscopic work[33] has further confirmed that the hydrated electron increases the range of motion of the nearby solvent molecules, consistent with a positive entropy of solvation. Thus, the solvation entropy is one of the key experimental observables that can help distinguish between proposed hydration structures of the hydrated electron from different simulation models.

Why have not researchers previously tried to reproduce the large positive solvation entropy of the $e^-_{hyd}$ from simulation? The reason is that calculating thermodynamic quantities from simulation is a highly nontrivial task, particularly for quantum mechanical objects like the hydrated electron. We accomplish this calculation by taking advantage of an alchemical simulation methodology (outlined in the Supporting Information) and a multistate free energy estimator.[34,35] We determine the solvation entropy for three one-electron models: the Turi-Borgis (TB) model,[19] which treats the electron as residing in a somewhat soft cavity; an optimized version of this model developed by our group, referred to as the TBOpt model,[20] which produces an even softer cavity that allows waters to partly penetrate into the electron density; and our previous noncavity model,[10] referred to as LGS, where water molecules reside within the electron density. Because of limited statistics associated with DFT-based simulations, we also determine the solvation entropy for the PBE0-D3 $e^-_{hyd}$ using several different methodologies, all of which agree within error.

We find that the two soft cavity-forming one-electron models give the correct sign of the solvation entropy but underestimate its magnitude, indicating that the predicted structures are in somewhat reasonable agreement with experiment. Both the noncavity and the hard-cavity PBE0-D3-based $e^-_{hyd}$ models give an incorrect negative sign for the solvation entropy. We note that given the difficulty in converging thermodynamic quantities for limited-statistics *ab initio* simulations,[36−39] our results are unable to pin down a precise numerical value for the solvation entropy of the PBE0-D3-simulated hydrated electron, but the agreement between our different approaches does allow us to conclude that the value is negative.

The fact that there has been no direct experimental measurement of the $e^-_{hyd}$'s structure has important implications both for chemical reactions involving this species[3,4,6] as well as for testing the different theoretical approaches that simulate its behavior.[10,14,15,19,20] Most theoretical work relies on the calculation of experimental observables that depend only indirectly on the solvation structure of the hydrated electron. Common observables include the absorption spectrum,[2,11,26] which is related to the radius of gyration of the electron's wave function,[2,40] the vertical binding energy (VBE),[2] which is measured by photoelectron spectroscopy,[41] and the partial molar volume, which also has been measured experimentally.[7,8,12,13]

Unfortunately, the absorption spectrum is not terribly sensitive to the details of the local hydration structure, as any structure that produces an electron with about the right size yields a spectrum in decent agreement with experiment. The VBE is challenging for *ab initio* simulations to compute because of subtleties with the zero of energy with periodic boundary conditions and the fact that it is difficult for DFT-based simulations to correctly predict the band gap of liquid water.[42] There also has been conflict between theory and experiment about how photoelectron spectra are corrected for scattering[41,43] and whether or not surface-bound electrons are present.[44] The partial molar volume, which is the volume change of a solution when one mole of solute is added, is perhaps the measure that is most directly connected to the hydration structure, but there is still no clear consensus as to which model, if any, provides the best match to experiment.[7,8,12,13]

The most common way to characterize the structure of a solvent around a solute is by examining the most probable solute−solvent distances. Figure 1(a) shows electron-oxygen radial distribution functions (RDFs), which plot the probability of finding the O atom of a water molecule at a given distance from the electron's center, for each of the four different $e^-_{hyd}$ models explored in this work. The two cavity-forming one-electron models (purple and blue curves) show generally broad and relatively unstructured RDFs, indicating that the nearby water molecules are free to sample many different distances from the hydrated electron's cavity. The noncavity model (green curve) shows that water can penetrate nearly all the way to the electron's center of mass, but is otherwise also quite unstructured. The DFT model (based on PBE0-D3, red curve), in contrast to all of the one-electron models, shows a sharply structured solvation environment with a well-defined cavity and three distinct solvation shell peaks where waters prefer to sit in relation to the electron. This type of solvation motif is characteristic of ions with negative solvation entropies, such as $Cl^-$, which strongly order the surrounding solvent and restrict solvent translational degrees of freedom.

In addition to ordering the distance at which solvent molecules sit, solutes can also restrict the orientations that solvent molecules can sample. Figures 1(b)−(e) show distributions of the angles taken by the dipole moments of the water molecules in the first solvation shells of the different hydrated electron models. The way we calculate this is defined in the Supporting Information (SI), and values around −0.7 indicate that a water molecule is coordinating the electron with a hydrogen pointing inward (i.e., H-bond solvation). The two cavity-forming one-electron models, and particularly the


https://doi.org/10.1021/acs.jpclett.5c02808
J. Phys. Chem. Lett. XXXX, XXX, XXX−XXX

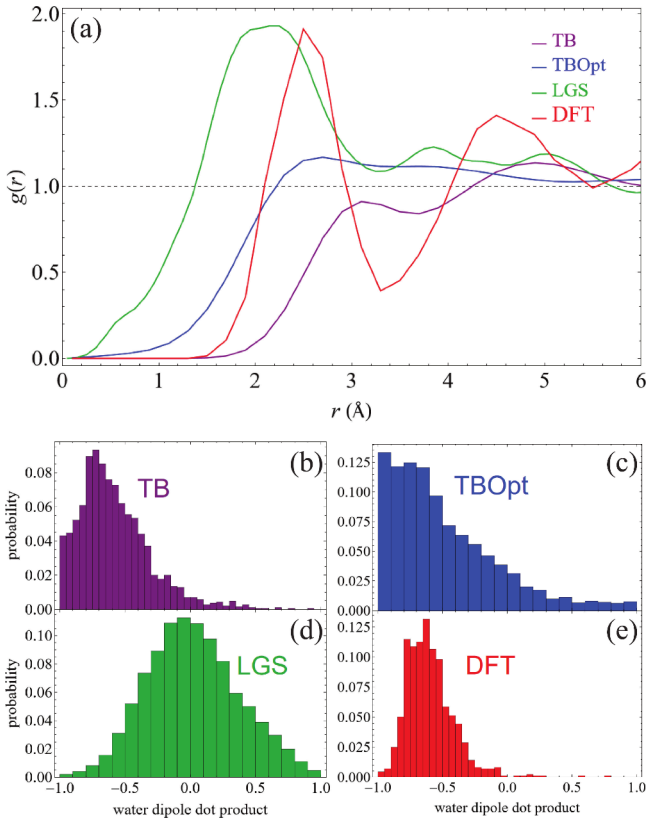


**Figure 1.** (A) Electron-water RDFs for different simulation models of the hydrated electron. The cavity-forming one-electron models (TB, purple; TBOpt, blue) show relatively unstructured 'soft' cavities; the noncavity model (LGS, green) allows water molecules to penetrate nearly to the center of the hydrated electron, while PBE0-D3 (red) yields a highly structured 'hard' cavity with a solvation structure more reminiscent of a small ion like $Cl^-$. Water dipole dot product distributions of the first-shell waters for the (B) TB, (C) TBOpt, (D) LGS, and (E) PBE0-D3 hydrated electron models. Here, a value of −1 means that the water dipole points toward the electron's center, a value of +1 means that the water oxygen points toward the electron's center, and a value of −0.7 means that a water H-bond points at the electron's center. The one-electron models show broader distributions of water-electron coordination angles while the PBE0-D3 model strongly orients the first-shell waters, again reminiscent of an ion like $Cl^-$.

TBOpt model, produce relatively broad water angular distributions, indicating that the first-shell water molecules can undergo a high degree of orientational fluctuations. The interior waters in the non-cavity-forming one-electron model have essentially random dipole orientations, as the waters in this model prefer to form H-bonds with themselves rather than with the $e^-_{hyd}$.[10] In contrast, the PBE0-D3-based DFT model shows a highly peaked distribution with a maximum value around −0.7, indicative of strong H-bond solvation and little flexibility in the orientations of the first-shell waters, again similar to what might be seen for an ion with negative solvation entropy like $Cl^-$.

Given the strong differences in the hydration structures of the different $e^-_{hyd}$ models, one would expect that they should also have different solvation entropies, $\Delta S_{solv}$. Calculating the solvation entropy from molecular dynamics simulations involves computing the way the free energy, $A$, of a system changes upon the addition of a solute to the solvent; once this free energy change is known from thermodynamic integration, described below, the solvation entropy can be calculated directly from the internal energy change, $\Delta U$ (which is directly available from the end-point simulations), using the definition of the Helmholtz free energy: $\Delta A = \Delta U - T\Delta S$. For simulations with limited statistics, such as those based on DFT, it can be difficult to pin down the equilibrium average value of $\Delta U$, which in turn limits the precision with which $\Delta S$ can be determined.

Given this difficulty, for our DFT-based $e^-_{hyd}$ simulations, we also have investigated an alternate approach that forgoes calculation of the internal energy. The idea is based on the fact that the entropy can also be expressed as a temperature derivative of the free energy: $S = -\left(\frac{\partial A}{\partial T}\right)_{N,V}$. Thus, by computing the solvation free energy at two different temperatures ($T - \Delta T$ and $T + \Delta T$), the entropy at temperature $T$ can be found from a finite-difference (FD) approach to this derivative:[45]

$$\Delta S(T) \simeq -\frac{\Delta A(T + \Delta T) - \Delta A(T - \Delta T)}{2\Delta T} \quad (1)$$

We note that this approach implicitly assumes that the heat capacity is constant over the range $2\Delta T$, which is an excellent approximation for our choice of water near room temperature with $\Delta T = 25$ K, as we assume here. Indeed, this range of $2\Delta T$ is known to be a conservative estimate for calculating aqueous solute solvation entropies.[45] We use neural network potentials (NNPs)[25] to compute the free energy at two different simulation temperatures. The NNP methodology we choose has precedent in the literature for modeling the temperature dependence[26] and other properties[27,28] of the hydrated electron.

Since thermodynamic quantities like the solvation entropy are state functions, the path over which we introduce the solute to the solvent to calculate the solvation free energy does not have to be physical. Thus, for our other approach to calculating $\Delta S$ of the $e^-_{hyd}$, we take advantage of an 'alchemical' methodology, where a $e^-_{hyd}$ is slowly grown (or equivalently annihilated) into a simulated box of pure water. This is done by defining a potential energy function that linearly interpolates between the potentials of two thermodynamic states, A and B:

$$U(\mathbf{r})_\lambda = U(\mathbf{r})_A \cdot \lambda + (1 - \lambda) \cdot U(\mathbf{r})_B \quad (2)$$

via a coupling parameter, $\lambda$. The solvation entropy is the entropy of transfer of an ideal gas-phase solute into a fully interacting solvent. Thus, state A corresponds to a gas-phase solute plus separate pure solvent system and state B corresponds to the interacting solution. Since the entropy of solvation is the entropy difference between these two end-states, it includes contributions from (i) how the electron changes the translational/rotational/vibrational degrees of freedom of nearby water molecules, and (ii) perturbation of the water−water interactions due to the nearby electron.

For our mixed quantum-classical simulations, we can directly scale the interaction between the classical waters and the quantum mechanical hydrated electron by linearly scaling the pseudopotential contribution to the potential energy. For *ab initio* DFT, this type of scheme is not feasible since there is no way straightforward way to decouple the potential between the water and excess electron from the total potential energy.


https://doi.org/10.1021/acs.jpclett.5c02808
J. Phys. Chem. Lett. XXXX, XXX, XXX−XXX

However, there is a straightforward approach to implementing eq 2 for *ab initio* simulations: at each time step of a DFT-based molecular dynamics simulation, a DFT calculation is done for both a pure water state and a hydrated electron state. The atomic forces and total energies of the simulation can then be taken as simple linear interpolations between these two end-point calculations. Unfortunately, this methodology is very computationally expensive, since $2\lambda$ DFT calculations must be done at every MD step for a pathway of $\lambda$ alchemical state points. There has been very recent work on Hamiltonian interpolation,[46] which necessitates only a single calculation per step per $\lambda$ state, however, this methodology is not yet widespread in quantum chemistry packages. In the SI, we present an additional methodology for recovering the solvation free energy of the PBE0-D3-based hydrated electron via an indirect thermodynamic cycle.[47,48] This method, which is hindered by one-sided averaging between DFT and a MQC simulation model, predicts a comparable free energy as our other methods.

Once an alchemical solvation simulation has been run, the free energy difference between the two end-states can be recovered by solving either the Bennett Acceptance Ratio (BAR) or the multistate Bennett Acceptance Ratio (MBAR) equations;[34,35,49] the free energy also can be obtained directly via thermodynamic integration (TI):[50,51]

$$\Delta A(B \rightarrow A) = \int_0^1 \left\langle \frac{\partial U}{\partial \lambda} \right\rangle_\lambda \mathrm{d}\lambda \tag{3}$$

For hydrated electrons, there is a subtlety with the choice of reference states.[31] In our implementation, the potential of the system when $\lambda = 0$ is that of pure water. But to compute solvation free energies, a better choice of reference state should be that of pure water plus an ideal gas solute that interacts with itself but not with the solvent. Of course, hydrated electrons do not exist in the absence of liquid water, so we have implicitly chosen the energy of the isolated gas-phase electron species to be zero. In the Supporting Information, we present calculations where we consider several other possible reference states, such as a free electron or an electron in a box, but we find that no matter what state we choose, these corrections make essentially no numerical difference to the final calculated entropy values.

We also note that it is typically difficult to compute solvation free energies for charged systems simulated with periodic boundary conditions.[15,52,53] This is because there is not a well-defined vacuum reference energy in periodic systems, so it is not possible to directly compare computed free energies with experiment unless significant finite-size corrections are applied.[15] In this work, however, we focus on the solvation entropy and not the free energy. The finite-size corrections for computing the solvation free energy at different temperatures, as well as for the internal energy, occur in the exact same way and do not have an entropic component. This means that when taking the difference between the free energy at different temperatures or the difference between the free and internal energies to calculate the solvation entropy, electrostatic finite-size effects precisely cancel. In the SI, we verify that even though our calculated free energy and internal energy values are sensitive to finite-size effects, as expected, the resulting calculated solvation entropy values are not. Since there are significant approximations involved in determining the magnitude of the finite-size free energy shifts, we choose not compare our free energy and internal energy values to other theoretical works that employ different approaches to account for finite-size corrections.[15,36]

Figure 2 shows the calculated solvation entropies for four different hydrated electron models as well as the experimental

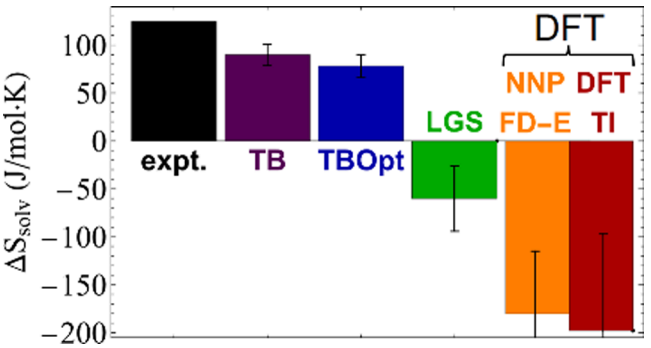


**Figure 2.** Solvation entropy values for different hydrated electron models (colored bars) in comparison to experimental values (black bar). The strongly positive experimental solvation entropy[31] indicates that the hydrated electron behaves like a hydrophobic ion (chaotrope). The soft cavity-forming one-electron models (TB; purple bar, TBOpt; blue bar) yield positive solvation entropies of the correct magnitude, although they underestimate the experimental value. The non-cavity-forming one-electron model (LGS; green bar) and the PBE0-D3 (orange and red bars) model produce qualitatively incorrect negative solvation entropies, which are typically associated with hydrophilic ions (kosmotropes) such as $Cl^-$. The orange bar shows the solvation entropy calculated using the FD approach[45] with NNPs,[25] while the red bar indicates the entropy calculated from *ab initio* TI[50] with an explicit calculation of the internal energy. Error bars are either raw standard deviations or estimates of the standard error from bootstrapping; convergence tests are detailed in the SI.

value (black bar). The cavity-forming one-electron models (purple and blue bars) predict the correct sign of $\Delta S$ but have magnitudes that underestimate the experimental value. This suggests that the $e^-_{hyd}$ produced from these models do not strongly orient or translationally restrict the waters around them, thus allowing for those waters to sample a variety of configurational states. However, these models do not allow the waters to sample as many configurations as would be seen experimentally. The noncavity (green bar) and PBE0-D3 (red bar from TI and orange bar from FD) hydrated electron models both predict a negative solvation entropy, which is qualitatively different from experiment.

The negative solvation entropy for the PBE0-D3 solvated electron makes sense, given that ions that show similarly structured aqueous solvation environments also have negative entropies of solvation.[31] This makes physical sense, as two solutes that disrupt the structure of liquid water in the same way, such as the PBE0-D3 $e^-_{hyd}$ and $Cl^-$, should yield similar $\Delta S_{solv}$'s. The negative $\Delta S$ produced by the noncavity LGS model likely has to do with the increased density of the water molecules inside the electron,[10] which restricts their freedom to diffuse and rotate relative to the bulk. Overall, our results indicate that both the PBE0-D3 and LGS hydrated electron models overly restrict the configurational degrees of freedom of the nearby solvent molecules relative to bulk water.[14]

Converging estimates of thermodynamic solvation quantities is notoriously challenging for DFT-based simulations[39,54] due to their computational cost, so that they provide only limited statistics from independent configurations. This is why the


https://doi.org/10.1021/acs.jpclett.5c02808
J. Phys. Chem. Lett. XXXX, XXX, XXX−XXX

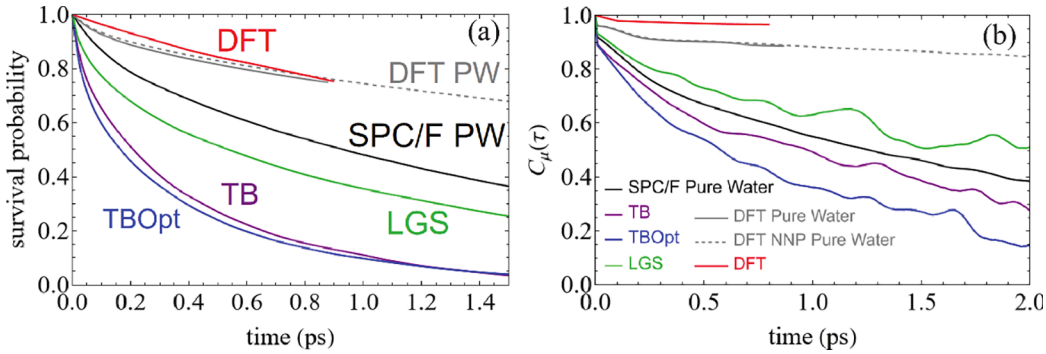


**Figure 3.** (A) Survival probabilities (SPs) for first-shell waters around different models of the hydrated electron (various colored curves) as well as those for pure classical SPC/Flex water (black curve) and pure PBE0-D3 water (solid gray curve). We also implemented a Behler-Parinello neural network[25,27] trained on pure water PBE0-D3 simulations to calculate these correlation functions out to longer times (dashed gray curves). It is clear that the long relaxation times are also reflected in the longer, NNP-based, simulations. The TB and TBOpt models (purple and blue curves, respectively) have SP decays that are much faster than those of bulk water, indicating that being near these electrons makes exchange of waters more facile, as expected for a solute with positive solvation entropy. The LGS (green curve) and PBE0-D3 (red curve) models have significantly slower survival probability decays, with waters near the PBE0-D3 electron exchanging more slowly than bulk PBE0-D3 waters. (B) First-shell water orientation autocorrelation functions for different hydrated electron models and pure water (same colors as panel A). The waters near the soft-cavity TB and TBOpt electrons are able to reorient more quickly than waters in bulk water, a chaotropic behavior consistent with a positive solvation entropy. The waters surrounding the noncavity LGS and hard-cavity PBE0-D3 hydrated electron models reorient more slowly than in the comparable bulk water, indicative of kosmotropic character associated with negative solvation entropy.

DFT-based PBE0-D3 $e^-_{hyd}$ solvation entropies (with both the TI method and NNP FD methods) shown in Figure 2 have much larger error bars than those for the one-electron models. As mentioned above, for the DFT TI methodology, most of the uncertainty comes from estimation of the $\Delta U$ from the end-point simulations.[51,55] In the SI, we present an analysis of several techniques for determining the uncertainty in the PBE0-D3 $e^-_{hyd}$ internal energy; we find that even with the most conservative error bars, the final calculated value of the solvation entropy must still be negative.

We note that our simulations are of similar or longer length compared to other DFT-based studies that compute solvation free energies of aqueous ions, and that our reported error bars are more conservative.[36−39,56,57] For the NNP FD method of computing $\Delta S$ for the PBE0-D3 $e^-_{hyd}$, the uncertainty depends only on the accuracy of the free energies at the two temperatures. With the longer NNP-based trajectories that can sample hundreds of uncorrelated configurations, this makes the net error bar for $\Delta S$ smaller than that based on the directly simulated free and internal energies. The error bar shown for the FD-based $\Delta S$ in Figure 2 uses the raw standard deviation for the uncertainties, which is the most generous error bar possible. Since limited statistics prevent us from pinning down a precise value, our main conclusion for the PBE0-D3 hydrated electron based on both the TI and NNP FD approaches is that its solvation entropy is negative.

To show that the different signs of the predicted solvation entropies of the different models make physical sense, we examined the translational and rotational motions of the first-shell water molecules around each of the different $e^-_{hyd}$ models. To do this, we first calculated survival probabilities (SPs) of waters in the first shell, which is the likelihood that a given water molecule in the first solvation shell remains in the first shell for some amount of time in the future. The decay of this measure indicates how long water molecules remain next to the $e^-_{hyd}$: a decay faster than that observed in bulk water indicates enhanced translational freedom, while a decay longer than that observed in bulk water indicates restricted translational motion. We also examined water orientation autocorrelation functions, $C_\mu(t)$, which measure how quickly the first-shell waters are able to reorient. This quantity is computed as $C_\mu(t) = \langle P_2[\hat{\mu}(0)\cdot\hat{\mu}(t)]\rangle$, where $P_2$ is the second-order Legendre polynomial and $\mu$ is a unit vector along the water O−H bond axis.

In general, it is known that aqueous ions with positive $\Delta S_{solv}$ tend to have waters that reorient more quickly than waters in the bulk (faster decay of $C_\mu(t)$), while ions with negative solvation entropies show slower reorientation of their first-shell waters.[32,58] Of course, the solvation entropy is not dictated solely by the way first-shell waters behave near the solute, however, there is a known connection between solvation entropy and the kosmotropic/chaotropic behavior of aqueous ions.[31] In other words, even though the solvation entropy is determined by the equilibrium solvation structure and not by dynamics, there is a strong correlation between the translational and rotational dynamics of the first-shell waters around aqueous ions, the value of $\Delta S_{solv}$, and as discussed further below, the position of an ion on the Hofmeister series.[32,58] Thus, we examine the first-shell water dynamics around each of our hydrated electron models to better contextualize our solvation entropy results.

Figure 3(a) shows SPs for the first-shell water molecules surrounding the different $e^-_{hyd}$ models (various colored curves), along with the average SP of waters in the bulk for SPC/Flex classical water (used in the one-electron simulations, black curve) and for PBE0-D3 water (solid gray curve). The two cavity-forming one-electron models both have first-shell SPs that decay faster than that of bulk water; the translational motion of these first-shell waters is enhanced by the presence of the electron. The noncavity model (green curve) has a decay that is also somewhat faster than bulk water, but is markedly slower than those of the two cavity models. For the PBE0-D3 $e^-_{aq}$ (red curve), the SP decay is slower than that seen in bulk PBE0-D3 water, something that is not consistent with the strongly positive experimental solvation entropy but which fits well with our calculation of a negative $\Delta S_{solv}$ for this model.


https://doi.org/10.1021/acs.jpclett.5c02808
J. Phys. Chem. Lett. XXXX, XXX, XXX−XXX

The orientation correlation functions, shown in Figure 3(b), indicate that the first-shell waters around the two cavity-forming one-electron models rotate faster than those in bulk water, consistent with their positive $\Delta S_{solv}$. This result is also consistent with recent experimental terahertz spectroscopy results[59] which show evidence for polaronic coupling between the hydrated electron and the librational modes of nearby water molecules. In contrast, the waters near both the PBE0-D3 and noncavity LGS models show restricted rotational motion relative to pure water. For PBE0-D3 in particular, this net restriction of rotational motion, which is consistent with the tight angular distributions in Figure 1e, makes perfect sense in light of the negative solvation entropy calculated for the PBE0-D3 hydrated electron. All of our results imply that the 'soft' cavity-forming TB and TBOpt one-electron models are doing a better job at qualitatively simulating the way the $e^-_{hyd}$ interacts with nearby water molecules than the noncavity LGS model or PBE0-D3. This result has broad implications for understanding the solution-phase behavior and reactivity of hydrated electrons, and strongly emphasizes that not all cavity structures are equivalent in terms of mapping simulations onto experimental observables.

One important chemical behavior that is particularly sensitive to the local hydration structure is ion pairing. The way aqueous ions interact with each other is captured by the Hofmeister series,[58] which orders ions from chaotropic (positive or weakly negative $\Delta S_{solv}$) to kosmotropic (very negative solvation entropies). Kosmotropes and chaotropes tend to pair with ions like themselves, so that studies of competitive ion pairing between different ions can help determine their position on the Hofmeister series.[58,60−63] For hydrated electrons, pairing with cations leads to a modest blue shift of the $e^-_{hyd}$'s absorption spectrum,[1,64,65] and indeed, for soft-cavity-forming one-electron models like TBOpt, chaotropic cations induce a larger spectral shift than kosmotropic cations.[61−63] This indicates that the electrons in these models are chaotropic, consistent with their positive $\Delta S_{solv}$ in Figure 2. In contrast, the PBE0-D3-simulated $e^-_{hyd}$ strongly overpairs with kosmotropic sodium cations, leading to a predicted spectral shift in the opposite direction of that seen experimentally.[14] Taken together, this all makes sense: PBE0-D3 produces a highly kosmotropic electron, which would prefer to strongly pair with kosmotropic cations like $Na^+$ even though experimentally little pairing is observed.[64,66]

In summary, we present explicit calculations of $\Delta S_{solv}$ for different simulation models of the $e^-_{hyd}$, and find that different models produce solvation entropies with different signs. This shows that even though a model produces a cavity hydrated electron, the local solvation structure may be qualitatively incorrect because not all cavity structures are equivalent. Hydrated electrons are champion chaotropes with a large, positive solvation entropy and thus interact with water molecules in a more hydrophobic rather than hydrophilic manner. Simulation models based on DFT using the PBE0-D3 functional, as well as a noncavity one-electron model, predict hydrated electrons with behavior that is more consistent with hydrophilic ion solvation, in contrast to experiment.[31] All of our solvation entropy results are consistent with both the structure and dynamics of the water molecules around the different hydrated electron models, as well as the way these models undergo ion pairing.

We note that to date, there is no single simulation model of the hydrated electron that correctly predicts all experimental observables. For example, although the TBOpt model correctly predicts a positive entropy of solvation, depending on the electrostatic calculation scheme being used, this model predicts an underestimated or negative partial molar volume, in contrast to experiment.[13,67] Conversely, PBE0-D3 DFT predicts a qualitatively correct, albeit significantly underestimated, partial molar volume,[12] but does not correctly predict the experimental absorption spectrum,[11,24,68] vertical detachment energy,[11] ion pairing[69] or transient hole-burning dynamics[23] of the hydrated electron. Each experimental observable probes slightly different aspects of the hydrated electron's solvation structure, and a holistic view of how a model predicts each of these measures is crucial for building a realistic understanding of $e^-_{hyd}$ simulation.

We note that DFT is not a systematically improvable level of theory, so one might expect that the use of different exchange-correlation functionals could have a large impact on simulation results for the $e^-_{hyd}$ system. However, dramatic changes in the solvation structure would be needed for the calculated $\Delta S_{solv}$ to reverse sign to become in qualitative agreement with experiment. To date, essentially every *ab initio* simulation of the hydrated electron[5,11,22,26,27] shows a highly structured solvation environment that is very similar to that presented here with the PBE0 exchange-correlation functional. In fact, we recently used numerous different density functionals to simulate the hydrated electron[24] and found that (except for functionals that led to a nonlocalized hydrated electron), the solvation structure was remarkably consistent across functionals spanning Jacob's Ladder.[30]

Overall, although our work does not pinpoint the precise hydration structure of the $e^-_{hyd}$, it does show that soft cavity-forming one-electron models produce a structure that is more consistent with experiment in terms of the entropy of solvation. The results suggest that these softer cavity models treat the electron in a more hydrophobic manner compared to PBE0-D3-based DFT and a noncavity pseudopotential model. Our work emphasizes that not all cavity models of the hydrated electron are equivalent, as different cavity structures can produce opposite signs for the predicted solvation entropy. We hope that this work inspires further investigation of the solvation structure of the hydrated electron, emphasizing that any good model must not only correctly predict the electron's absorption spectrum, vertical detachment energy and molar solvation volume, but also the strongly positive solvation entropy.

## ■ ASSOCIATED CONTENT

### Data Availability Statement

All data and necessary files were uploaded to a Dryad repository (DOI: 10.5061/dryad.931zcrjw5), which is freely accessible. The repository contains all energy files necessary for the free energy calculations as well as the files needed to run the DFT-based simulations. A python notebook is also included which gives an example for calculating the solvation entropy for one of the one-electron models used in this work. All trajectory files or sampled atomic configurations are included as well.

### Supporting Information

The Supporting Information is available free of charge at https://pubs.acs.org/doi/10.1021/acs.jpclett.5c02808.



https://doi.org/10.1021/acs.jpclett.5c02808
J. Phys. Chem. Lett. XXXX, XXX, XXX−XXX

Methods, alchemical solvation, DFT solvation entropy calculations by thermodynamic integration and thermodynamic cycle, integration method dependence, equilibration convergence analysis, DFT $e^-_{hyd}$solvation entropy by the FD method, finite-size effects and electrostatic corrections, corrections for the decoupled electron reference state, and water structural and dynamic measures (PDF)

## AUTHOR INFORMATION


### Corresponding Author

**Benjamin J. Schwartz** − *Department of Chemistry and Biochemistry, University of California, Los Angeles, California 90095, United States;* orcid.org/0000-0003-3257-9152; Email: bjs@g.ucla.edu

### Authors

**William R. Borrelli** − *Department of Chemistry and Biochemistry, University of California, Los Angeles, California 90095, United States*

**Xiaoyan Liu** − *Department of Chemistry and Biochemistry, University of California, Los Angeles, California 90095, United States*

Complete contact information is available at: https://pubs.acs.org/10.1021/acs.jpclett.5c02808


### Notes

The authors declare no competing financial interest.

## ACKNOWLEDGMENTS

This work was supported by the National Science Foundation, under Grant CHE-2247583. Partial support for W.R.B. was provided by the U.S. Department of Energy, Basic Energy Sciences Condensed-Phase and Interfacial Molecular Science Program, under Grant DE-SC0017800. Computational resources were provided by the University of California, Los Angeles (UCLA) Institute for Digital Research and Education and Extreme Science and Engineering Discovery Environment (XSEDE), under Computational Project TG-CHE170065. The authors would like to Sanghyun Park and Kenneth J. Mei for their insightful discussions over the course of this work.

## REFERENCES


(1) Hart, E. J.; Boag, J. W. Absorption Spectrum of the Hydrated Electron in Water and in Aqueous Solutions. *J. Am. Chem. Soc.* **1962**, *84*, 4090−4095.

(2) Herbert, J. M. Structure of the aqueous electron. *Phys. Chem. Chem. Phys.* **2019**, *21*, 20538−20565.

(3) Borrelli, W. R.; Guardado Sandoval, J. L.; Mei, K. J.; Schwartz, B. J. Roles of H-Bonding and Hydride Solvation in the Reaction of Hydrated (Di)electrons with Water to Create H2 and OH−. *J. Chem. Theory Comput.* **2024**, *20* (16), 7337−7346.

(4) Neupane, P.; Bartels, D. M.; Thompson, W. H. Exploring the Unusual Reactivity of the Hydrated Electron with CO2. *J. Phys. Chem. B* **2024**, *128*, 567−575.

(5) Marsalek, O.; Uhlig, F.; VandeVondele, J.; Jungwirth, P. Structure, Dynamics, and Reactivity of Hydrated Electrons by Ab Initio Molecular Dynamics. *Acc. Chem. Res.* **2012**, *45*, 23−32.

(6) Rybkin, V. V. Mechanism of Aqueous Carbon Dioxide Reduction by the Solvated Electron. *J. Phys. Chem. B* **2020**, *124*, 10435−10441.

(7) Borsarelli, C. D.; Bertolotti, S. G.; Previtali, C. M. Thermodynamic changes associated with the formation of the hydrated electron after photoionization of inorganic anions: a time-resolved photoacoustic study. *Photochemical and Photobiological Sciences* **2003**, *2*, 791−795.

(8) Janik, I.; Lisovskaya, A.; Bartels, D. M. Partial Molar Volume of the Hydrated Electron. *J. Phys. Chem. Lett.* **2019**, *10*, 2220−2226.

(9) Novelli, F.; Chen, K.; Buchmann, A.; Ockelmann, T.; Hoberg, C.; Head-Gordon, T.; Havenith, M. The birth and evolution of solvated electrons in the water. *Proc. Natl. Acad. Sci. U.S.A.* **2023**, *120* (8), No. e2216480120.

(10) Larsen, R. E.; Glover, W. J.; Schwartz, B. J. Does the Hydrated Electron Occupy a Cavity? *Science* **2010**, *329*, 65−69.

(11) Park, S. J.; Schwartz, B. J. Understanding the Temperature Dependence and Finite Size Effects in Ab Initio MD Simulations of the Hydrated Electron. *J. Chem. Theory Comput.* **2022**, *18*, 4973−4982.

(12) Borrelli, W. R.; Mei, K. J.; Park, S. J.; Schwartz, B. J. Partial Molar Solvation Volume of the Hydrated Electron Simulated Via DFT. *J. Phys. Chem. B* **2024**, *128*, 2425−2431.

(13) Neupane, P.; Bartels, D. M.; Thompson, W. H. Relation between the Hydrated Electron Solvation Structure and Its Partial Molar Volume. *J. Phys. Chem. B* **2023**, *127*, 5941.

(14) Park, S. J.; Narvaez, W. A.; Schwartz, B. J. Ab Initio Studies of Hydrated Electron/Cation Contact Pairs: Hydrated Electrons Simulated with Density Functional Theory Are Too Kosmotropic. *J. Phys. Chem. Lett.* **2023**, *14*, 559−566.

(15) Ambrosio, F.; Miceli, G.; Pasquarello, A. Electronic Levels of Excess Electrons in Liquid Water. *J. Phys. Chem. Lett.* **2017**, *8*, 2055−2059.

(16) Marcus, R. A. Theory of Electron-Transfer Reaction Rates of Solvated Electrons. *J. Chem. Phys.* **1965**, *43*, 3477−3489.

(17) Neupane, P.; Katiyar, A.; Bartels, D. M.; Thompson, W. H. Investigation of the Failure of Marcus Theory for Hydrated Electron Reactions. *J. Phys. Chem. Lett.* **2022**, *13*, 8971−8977.

(18) Hammer, N. I.; Shin, J.-W.; Headrick, J. M.; Diken, E. G.; Roscioli, J. R.; Weddle, G. H.; Johnson, M. A. How Do Small Water Clusters Bind an Excess Electron? *Science* **2004**, *306*, 675−679.

(19) Turi, L.; Gaigeot, M.-P.; Levy, N.; Borgis, D. Analytical investigations of an electron-water molecule pseudopotential. I. Exact calculations on a. *model system* **2001**, *114*, 7805−7815.

(20) Glover, W. J.; Schwartz, B. J. Short-Range Electron Correlation Stabilizes Noncavity Solvation of the Hydrated Electron. *J. Chem. Theory Comput.* **2016**, *12*, 5117−5131.

(21) Rossky, P. J.; Schnitker, J. The hydrated electron: quantum simulation of structure, spectroscopy, and dynamics. *J. Phys. Chem.* **1988**, *92*, 4277−4285.

(22) Uhlig, F.; Marsalek, O.; Jungwirth, P. Unraveling the Complex Nature of the Hydrated Electron. *J. Phys. Chem. Lett.* **2012**, *3*, 3071−3075.

(23) Park, S. J.; Schwartz, B. J. How Ions Break Local Symmetry: Simulations of Polarized Transient Hole Burning for Different Models of the Hydrated Electron in Contact Pairs with Na+. *J. Phys. Chem. Lett.* **2023**, *14*, 3014−3022.

(24) Borrelli, W. R.; Liu, X.; Schwartz, B. J. How the choice of exchange−correlation functional affects DFT-based simulations of the hydrated electron. *J. Chem. Phys.* **2025**, *162*, 110901.

(25) Behler, J.; Parrinello, M. Generalized Neural-Network Representation of High-Dimensional Potential-Energy Surfaces. *Phys. Rev. Lett.* **2007**, *98*, 146401.

(26) Lan, J.; Rybkin, V. V.; Pasquarello, A. Temperature Dependent Properties of the Aqueous Electron. *Angew. Chem. Int. Ed.* **2022**, *61*, e202209398.

(27) Lan, J.; Kapil, V.; Gasparotto, P.; Ceriotti, M.; Iannuzzi, M.; Rybkin, V. V. Simulating the ghost: quantum dynamics of the solvated electron. *Nat. Commun.* **2021**, *12*, 766.

(28) Gao, R.; Li, Y.; Car, R. Enhanced deep potential model for fast and accurate molecular dynamics: application to the hydrated electron. *Phys. Chem. Chem. Phys.* **2024**, *26*, 23080−23088.

(29) Johnson, E. R.; Otero-de-la Roza, A.; Dale, S. G. Extreme density-driven delocalization error for a model solvated-electron system. *J. Chem. Phys.* **2013**, *139*, 184116.
(30) Perdew, J. P.; Schmidt, K. Jacob's ladder of density functional approximations for the exchange-correlation energy. *AIP Conf. Proc.* **2001**, *577*, 1−20.
(31) Han, P.; Bartels, D. M. On the hydrated electron as a structure-breaking ion. *J. Phys. Chem.* **1991**, *95*, 5367−5370.
(32) Bakker, H. J. Structural Dynamics of Aqueous Salt Solutions. *Chem. Rev.* **2008**, *108*, 1456−1473.
(33) Novelli, F.; Chen, K.; Buchmann, A.; Ockelmann, T.; Hoberg, C.; Head-Gordon, T.; Havenith, M. The birth and evolution of solvated electrons in the water. *Proc. Natl. Acad. Sci. U. S. A.* **2023**, *120*, No. e2216480120.
(34) Bennett, C. H. Efficient estimation of free energy differences from Monte Carlo data. *J. Comput. Phys.* **1976**, *22*, 245−268.
(35) Shirts, M. R.; Chodera, J. D. Statistically optimal analysis of samples from multiple equilibrium states. *J. Chem. Phys.* **2008**, *129*, 124105.
(36) Gao, L.; Zhang, L.; Fu, Q.; Bu, Y. Molecular Dynamics Characterization of Dielectron Hydration in Liquid Water with Unique Double Proton Transfers. *J. Chem. Theory Comput.* **2021**, *17*, 666−677.
(37) Shi, Y.; Beck, T. L. Absolute ion hydration free energy scale and the surface potential of water via quantum simulation. *Proc. Natl. Acad. Sci. U. S. A.* **2020**, *117*, 30151−30158.
(38) Prasetyo, N.; Hünenberger, P. H.; Hofer, T. S. Single-Ion Thermodynamics from First Principles: Calculation of the Absolute Hydration Free Energy and Single-Electrode Potential of Aqueous Li+ Using ab Initio Quantum Mechanical/Molecular Mechanical Molecular Dynamics Simulations. *J. Chem. Theory Comput.* **2018**, *14*, 6443−6459.
(39) Lin, C.; He, X.; Xi, C.; Zhang, Q.; Wang, L.-W. Ion solvation free energy calculations based on first-principles molecular dynamics thermodynamic integration. *J. Chem. Phys.* **2024**, *160*, 184115.
(40) Bartels, D. M. Moment analysis of hydrated electron cluster spectra: Surface or internal states? *J. Chem. Phys.* **2001**, *115*, 4404−4405.
(41) Luckhaus, D.; Yamamoto, Y.-i.; Suzuki, T.; Signorell, R. Genuine binding energy of the hydrated electron. *Science Advances* **2017**, *3*, No. e1603224.
(42) Bischoff, T.; Reshetnyak, I.; Pasquarello, A. Band gaps of liquid water and hexagonal ice through advanced electronic-structure calculations. *Phys. Rev. Res.* **2021**, *3*, 023182.
(43) Bartels, D. M. Is the Hydrated Electron Vertical Detachment Genuinely Bimodal? *J. Phys. Chem. Lett.* **2019**, *10*, 4910−4913.
(44) Siefermann, K. R.; Liu, Y.; Lugovoy, E.; Link, O.; Faubel, M.; Buck, U.; Winter, B.; Abel, B. Binding energies, lifetimes and implications of bulk and interface solvated electrons in water. *Nat. Chem.* **2010**, *2*, 274−279.
(45) Kubo, M. M.; Gallicchio, E.; Levy, R. M. Thermodynamic Decomposition of Hydration Free Energies by Computer Simulation: Application to Amines, Oxides, and Sulfides. *J. Phys. Chem. B* **1997**, *101*, 10527−10534.
(46) Li, C.; Zhang, X.; Chan, G. K.-L. General Quantum Alchemical Free Energy Simulations via Hamiltonian Interpolation. *J. Chem. Theory Comput.* **2025**, *21*, 6644−6652.
(47) Giese, T. J.; York, D. M. Development of a Robust Indirect Approach for MM → QM Free Energy Calculations That Combines Force-Matched Reference Potential and Bennett's Acceptance Ratio Methods. *J. Chem. Theory Comput.* **2019**, *15*, 5543−5562.
(48) Gao, J. Absolute free energy of solvation from Monte Carlo simulations using combined quantum and molecular mechanical potentials. *J. Phys. Chem.* **1992**, *96*, 537−540.
(49) Shirts, M.; et al. choderalab/pymbar: 4.0.3 Support for Python 3.12 and Jax 0.3.25+. *Zenodo* **2024**, DOI: 10.5281/zenodo.10849928.
(50) Kirkwood, J. G. Statistical Mechanics of Fluid Mixtures. *J. Chem. Phys.* **1935**, *3*, 300−313.
(51) Duarte Ramos Matos, G.; Kyu, D. Y.; Loeffler, H. H.; Chodera, J. D.; Shirts, M. R.; Mobley, D. L. Approaches for Calculating Solvation Free Energies and Enthalpies Demonstrated with an Update of the FreeSolv Database. *J. Chem. Eng. Data* **2017**, *62*, 1559−1569.
(52) Ambrosio, F.; Miceli, G.; Pasquarello, A. Redox levels in aqueous solution: Effect of van der Waals interactions and hybrid functionals. *J. Chem. Phys.* **2015**, *143*, 244508.
(53) Komsa, H.-P.; Rantala, T. T.; Pasquarello, A. Finite-size supercell correction schemes for charged defect calculations. *Phys. Rev. B* **2012**, *86*, 045112.
(54) Duignan, T. T.; Baer, M. D.; Schenter, G. K.; Mundy, C. J. Real single ion solvation free energies with quantum mechanical simulation. *Chem. Sci.* **2017**, *8*, 6131−6140.
(55) Roy, A.; Hua, D. P.; Ward, J. M.; Post, C. B. Relative Binding Enthalpies from Molecular Dynamics Simulations Using a Direct Method. *J. Chem. Theory Comput.* **2014**, *10*, 2759−2768.
(56) Xi, C.; Zheng, F.; Gao, G.; Song, Z.; Zhang, B.; Dong, C.; Du, X.-W.; Wang, L.-W. Ion Solvation Free Energy Calculation Based on Ab Initio Molecular Dynamics Using a Hybrid Solvent Model. *J. Chem. Theory Comput.* **2022**, *18*, 6878−6891.
(57) Shi, Y.; Beck, T. L. Absolute ion hydration free energy scale and the surface potential of water via quantum simulation. *Proc. Natl. Acad. Sci. U. S. A.* **2020**, *117*, 30151−30158.
(58) Borkowski, A. K.; Piskulich, Z. A.; Thompson, W. H. Examining the Hofmeister Series through Activation Energies: Water Diffusion in Aqueous Alkali-Halide Solutions. *J. Phys. Chem. B* **2021**, *125*, 350−359.
(59) Woerner, M.; Fingerhut, B. P.; Elsaesser, T. Field-Induced Electron Generation in Water: Solvation Dynamics and Many-Body Interactions. *J. Phys. Chem. B* **2022**, *126*, 2621−2634.
(60) Marcus, Y. Effect of Ions on the Structure of Water: Structure Making and Breaking. *Chem. Rev.* **2009**, *109*, 1346−1370.
(61) Liu, H. Y.; Mei, K. J.; Borrelli, W. R.; Schwartz, B. J. Simulating the Competitive Ion Pairing of Hydrated Electrons with Chaotropic Cations. *J. Phys. Chem. B* **2024**, *128*, 8557−8566.
(62) Narvaez, W. A.; Park, S. J.; Schwartz, B. J. Competitive Ion Pairing and the Role of Anions in the Behavior of Hydrated Electrons in Electrolytes. *J. Phys. Chem. B* **2022**, *126*, 7701−7708.
(63) Narvaez, W. A.; Park, S. J.; Schwartz, B. J. Hydrated Electrons in High-Concentration Electrolytes Interact with Multiple Cations: A Simulation Study. *J. Phys. Chem. B* **2022**, *126*, 3748−3757.
(64) Bonin, J.; Lampre, I.; Mostafavi, M. Absorption spectrum of the hydrated electron paired with nonreactive metal cations. *Radiat. Phys. Chem.* **2005**, *74*, 288−296.
(65) Dobrovolskii, D.; Mostafavi, M.; Denisov, S. A. Solvation dynamics of electron−metal cation contact pairs in LiCl aqueous solutions. *Phys. Chem. Chem. Phys.* **2025**, *27*, 14070−14074.
(66) Narvaez, W. A.; Wu, E. C.; Park, S. J.; Gomez, M.; Schwartz, B. J. Trap-Seeking or Trap-Digging? Photoinjection of Hydrated Electrons into Aqueous NaCl Solutions. *J. Phys. Chem. Lett.* **2022**, *13*, 8653−8659.
(67) Neupane, P.; Bartels, D. M.; Thompson, W. H. Empirically Optimized One-Electron Pseudopotential for the Hydrated Electron: A Proof-of-Concept Study. *J. Phys. Chem. B* **2023**, *127*, 7361−7371.
(68) Uhlig, F.; Herbert, J. M.; Coons, M. P.; Jungwirth, P. Optical Spectroscopy of the Bulk and Interfacial Hydrated Electron from Ab Initio Calculations. *J. Phys. Chem. A* **2014**, *118*, 7507−7515.
(69) Park, S. J.; Schwartz, B. J. How Ions Break Local Symmetry: Simulations of Polarized Transient Hole Burning for Different Models of the Hydrated Electron in Contact Pairs with Na+. *J. Phys. Chem. Lett.* **2023**, *14*, 3014−3022.


https://doi.org/10.1021/acs.jpclett.5c02808
J. Phys. Chem. Lett. XXXX, XXX, XXX−XXX